# Crystal structure of the activated insulin receptor tyrosine kinase in complex with peptide substrate and ATP analog

## Stevan R.Hubbard

Department of Pharmacology and Skirball Institute of Biomolecular Medicine, 540 First Avenue, New York University Medical Center, New York, NY 10016, USA

e-mail: hubbard@tallis.med.nyu.edu

**The crystal structure of the phosphorylated, activated form of the insulin receptor tyrosine kinase in complex with a peptide substrate and an ATP analog has been determined at 1.9 Å resolution. The activation loop (A-loop) of the kinase undergoes a major conformational change upon autophosphorylation of Tyr1158, Tyr1162 and Tyr1163 within the loop, resulting in unrestricted access of ATP and protein substrates to the kinase active site. Phosphorylated Tyr1163 (pTyr1163) is the key phosphotyrosine in stabilizing the conformation of the tris-phosphorylated A-loop, whereas pTyr1158 is completely solvent-exposed, suggesting an availability for interaction with downstream signaling proteins. The YMXM-containing peptide substrate binds as a short anti-parallel β-strand to the C-terminal end of the A-loop, with the methionine side chains occupying two hydrophobic pockets on the C-terminal lobe of the kinase. The structure thus reveals the molecular basis for insulin receptor activation via autophosphorylation, and provides insights into tyrosine kinase substrate specificity and the mechanism of phosphotransfer.**

*Keywords*: autophosphorylation/insulin receptor/protein tyrosine kinase/substrate specificity/ X-ray crystallography

## Introduction

Insulin stimulates numerous intracellular signaling pathways that regulate cellular metabolism and growth (White and Kahn, 1994). The physiological effects of insulin are mediated by its cell surface receptor, an $\alpha_2\beta_2$ transmembrane glycoprotein with intrinsic protein tyrosine kinase activity (Ebina *et al.*, 1985; Ullrich *et al.*, 1985). Binding of insulin to the extracellular α-chains results in autophosphorylation of specific tyrosine residues in the cytoplasmic portion of the β-chains: two in the juxtamembrane region, three in the kinase (catalytic) domain, and two in the C-terminal tail (Tornqvist *et al.*, 1987; Tavare *et al.*, 1988; White *et al.*, 1988; Feener *et al.*, 1993; Kohanski, 1993). Autophosphorylation of Tyr1158, Tyr1162 and Tyr1163 in the activation loop (A-loop) of the kinase domain is critical for stimulation of kinase activity and biological function (Rosen *et al.*, 1983; Ellis *et al.*, 1986).

The vast majority of receptor tyrosine kinases contain between one and three tyrosine residues in the kinase A-loop, which comprises subdomains VII and VIII of the protein kinase catalytic core (Hanks *et al.*, 1991). In addition to the insulin receptor, other receptor tyrosine kinases whose biological function has been shown to depend on tyrosine autophosphorylation in the A-loop include insulin-like growth factor 1 (IGF-1) receptor (Kato *et al.*, 1994), fibroblast growth factor (FGF) receptor (Mohammadi *et al.*, 1996a), hepatocyte growth factor receptor (MET) (Longati *et al.*, 1994), nerve growth factor receptor (TRKA) (Mitra, 1991), and brain-derived neurotrophic factor receptor (TRKB) (Middlemas *et al.*, 1994).

The crystal structure of the unphosphorylated, low activity form of the insulin receptor kinase domain (IRK) has been reported previously (Hubbard *et al.*, 1994). This structure suggested an autoinhibitory mechanism whereby Tyr1162 in the A-loop competes with protein substrates for binding in the active site, while residues in the beginning of the A-loop restrict access to ATP such that *cis*-autophosphorylation of Tyr1162 is prevented. Here, the crystal structure at 1.9 Å resolution of the tris-phosphorylated, activated form of IRK (IRK3P) in complex with a peptide substrate and an ATP analog is presented. The conformational changes that occur upon autophosphorylation provide an understanding at the molecular level of the role of autophosphorylation in the activation of the insulin receptor and presumably other receptor tyrosine kinases. Moreover, the structure reveals the mode of peptide substrate binding to the insulin receptor kinase, and affords insights into the phosphotransfer mechanism.

## Results and discussion

### Structure determination

A 306-residue fragment of the β-chain of the human insulin receptor which possesses tyrosine kinase activity was produced in a baculovirus/insect cell expression system (Wei *et al.*, 1995). Cytoplasmic residues that are not included in the expressed protein are the first 25 (juxtamembrane region) and the last 72 (C-terminal tail). Addition of MgATP to the purified kinase results in autophosphorylation of Tyr1158, Tyr1162 and Tyr1163 as confirmed by mass spectrometry and microsequencing of tryptic peptides (Wei *et al.*, 1995). Crystals belonging to trigonal space group P3$_2$21 were obtained from a ternary complex consisting of IRK3P, an 18-residue peptide substrate and a non-hydrolyzable ATP analog, adenylyl imidodiphosphate (AMP-PNP).

The structure of the ternary complex was solved by molecular replacement using the structure of IRK as a search model, and has been refined at 1.9 Å resolution with a crystallographic *R*-value of 19.6% (6.0–1.9 Å, F>2σ). The atomic model includes all but the three N-terminal residues of IRK3P, one AMP-PNP molecule,
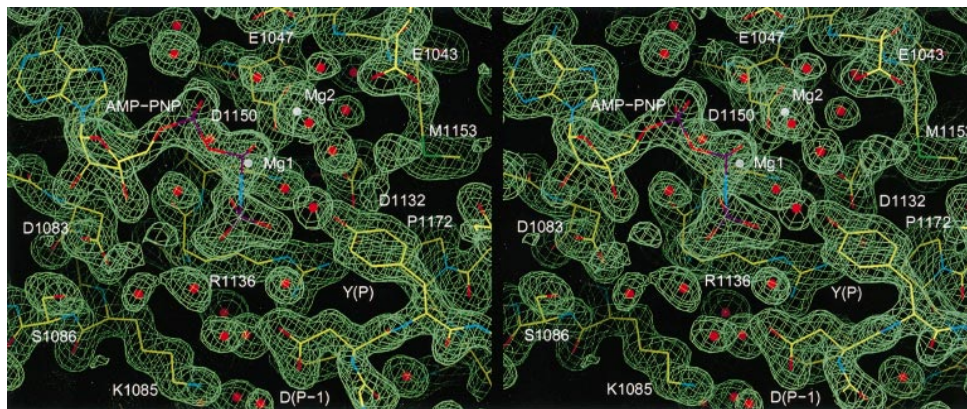
**Fig. 1.** Electron density map of the active site of IRK3P. Stereo view of a $2F_o–F_c$ map computed at 1.9 Å resolution and contoured at 1.2σ. Superimposed is the refined atomic model. Carbon atoms are yellow, oxygen atoms red, nitrogen atoms blue, phosphate atoms purple, and sulfur atoms green. The red spheres represent water molecules and the white spheres represent $Mg^{2+}$ ions. Figure prepared with SETOR (Evans, 1993).

**Table I.** Data collection and refinement summary

| Data collection | | | | | |
| --- | --- | --- | --- | --- | --- |
| Resolution (Å) | Observations (N) | Completeness (%) | Redundancy (%) | $R_{sym}$ (%)[a] | Signal ⟨$I/\sigma(I)$⟩ |
| 20.0–1.9 | 93535 | 98.6 (90.6)[b] | 4.1 | 6.5 (15.3)[b] | 12.9 |

| Refinement[c] | | | | | |
| --- | --- | --- | --- | --- | --- |
| Resolution (Å) | Reflections (N) | $R$-value (%)[d] | Root-mean-square deviations | | |
| | | | Bonds (Å) | Angles (°) | B-factors (Å$^2$)[e] |
| 6.0–1.9 | 25082 | 19.4 (22.6)[f] | 0.008 | 1.5 | 1.4 |

[a]$R_{sym} = 100 \times \Sigma_{hkl}\Sigma_i | I_i(hkl)–\langle I(hkl)\rangle |/\Sigma_{hkl}\Sigma_i I_i(hkl)$.
[b]Value in parentheses is for the highest resolution shell.
[c]Atomic model includes 303 IRK3P residues, six peptide residues, one AMP-PNP molecule, two $Mg^{2+}$ ions, 202 water molecules (2653 atoms).
[d]$R$-value $= 100 \times \Sigma_{hkl} | F_o(hkl)|–|F_c(hkl)| |/\Sigma_{hkl}|F_o(hkl)|$, where $F_o$ and $F_c$ are the observed and calculated structure factors, respectively ($F_o > 2\sigma$).
[e]For bonded protein atoms.
[f]Value in parentheses is the free $R$-value determined from 5% of the data.

two $Mg^{2+}$ ions, six residues of the peptide substrate and 202 water molecules. An electron density map in the vicinity of the active site is shown in Figure 1, data collection and refinement statistics are given in Table I, and a ribbon diagram of ternary IRK3P is shown in Figure 2A.

### Activation loop conformation

In the unliganded IRK structure determined previously (Hubbard *et al.*, 1994), the A-loop (residues 1149–1170) traverses the cleft between the N- and C-terminal lobes such that both protein substrate and ATP binding sites are occupied. Tyr1162 in the A-loop is bound in the active site, hydrogen-bonded to the putative catalytic base (Asp1132), and residues of the protein kinase-conserved [1150]DFG sequence in the beginning of the A-loop occupy the ATP binding site. Autophosphorylation of Tyr1158, Tyr1162 and Tyr1163 results in a dramatic change in the conformation of the A-loop (Figures 2B and 4A). Tyr1158, for example, is displaced ~30 Å from its position in the unphosphorylated A-loop. The conformation of the tris-phosphorylated A-loop permits unrestricted access to the binding sites for ATP and protein substrates.

The tris-phosphorylated A-loop is stabilized to various extents by the phosphotyrosine (pTyr) residues (Figure 4B). The phosphate group of pTyr1163 bridges the A-loop via hydrogen bonds to the side chain of Arg1155 on one side of the loop and to the backbone amide nitrogen of Gly1166 on the other side. In addition to the electrostatic interaction with Arg1155, the phenolic ring of pTyr1163 is packed against the aliphatic portion of the Arg1155 side chain. Arg1155 is also hydrogen-bonded to the carbonyl oxygen of the preceding residue. Arginine or lysine is highly conserved in the tyrosine kinase family at this position. The phosphate group of pTyr1162 makes two hydrogen bonds to the side chain of Arg1164. For receptor tyrosine kinases with tandem tyrosine residues corresponding to Tyr1162 and Tyr1163 (e.g. TRK, FGF receptor), an arginine or lysine is often found at the Arg1164 position. The phosphate group of pTyr1158 makes no protein contacts and consequently is the least ordered of the three phosphate groups.

Two short β-strand interactions also serve to stabilize the tris-phosphorylated A-loop. β9 in the A-loop is paired with β6, which precedes the catalytic loop (residues 1130–1137), and β10 in the A-loop is paired with β12 between αEF and αF (Figures 2A and 3). This pairing scheme leaves β11, which in IRK was paired with β10, available
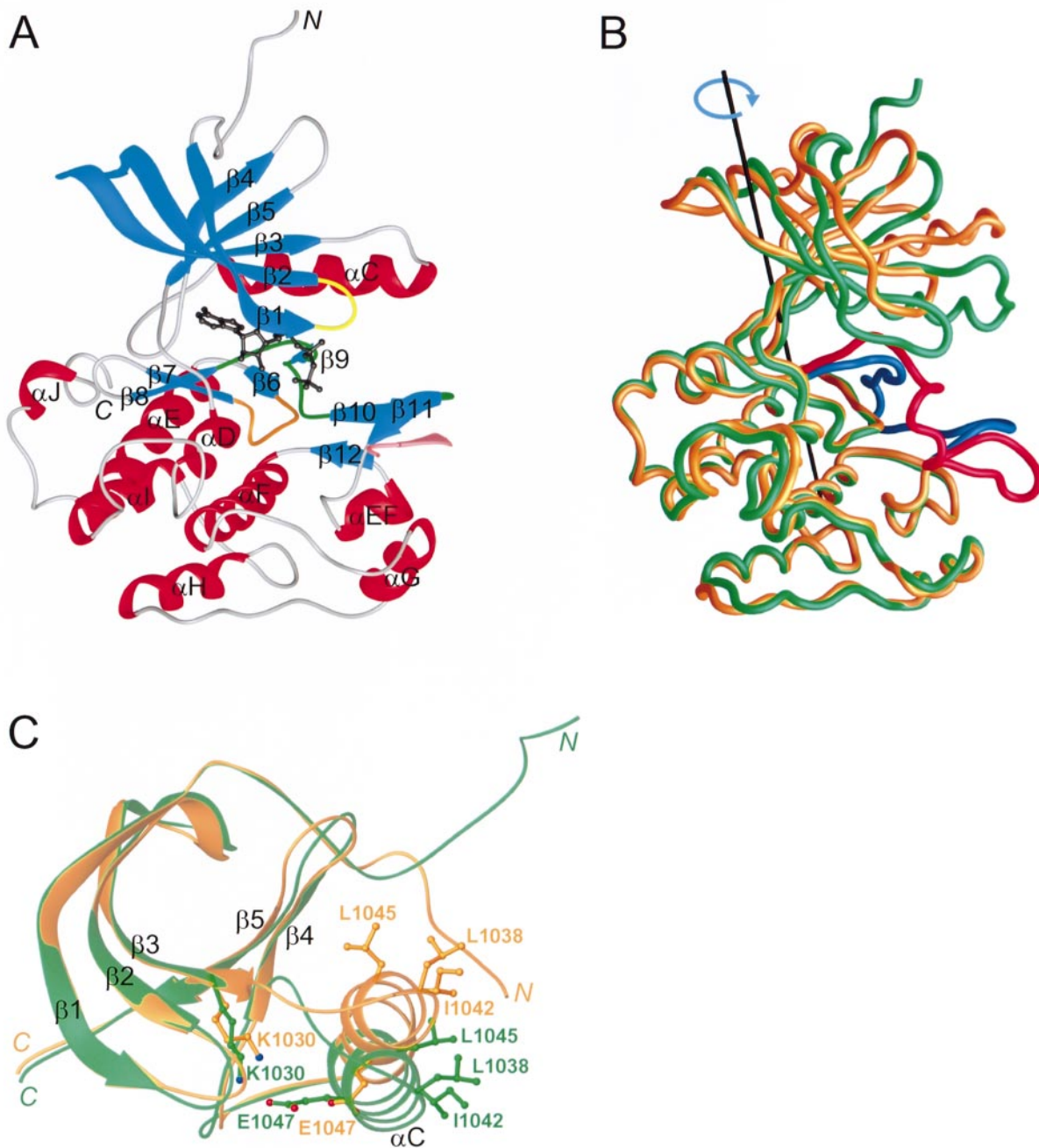
Fig. 2. Overall view of IRK3P and comparison with IRK. (**A**) Ribbon diagram of the IRK3P structure. The α-helices are shown in red, the β-strands in blue, the nucleotide-binding loop in yellow, the catalytic loop in orange, the activation loop in green, AMP-PNP in black and the peptide substrate in pink. The termini are denoted by N and C. (**B**) Superposition of the C-terminal lobes of IRK and IRK3P. The backbone representation of IRK/IRK3P is colored orange/green, with the activation loop colored red/blue. The axis (black) and arrow (blue) specify the rotation required to align the N-terminal β-sheet of IRK with that of IRK3P. (**C**) Superposition of the β-sheets in the N-terminal lobes of IRK and IRK3P. The backbone representation and carbon atoms of IRK/IRK3P are colored orange/green, oxygen atoms are red and nitrogen atoms are blue. (A) and (C) prepared with RIBBONS (Carson, 1991), (B) with GRASP (Nicholls *et al.*, 1991).

for interaction with a protein substrate. Compared with the unphosphorylated A-loop, which was poorly ordered for residues 1152–1157, the tris-phosphorylated A-loop is relatively well ordered.

The conformation of the tris-phosphorylated A-loop is in general similar to that of the mono-phosphorylated A-loop of cyclic AMP-dependent protein kinase (cAPK) (Knighton *et al.*, 1991), cyclin-dependent kinase 2 (CDK2) (Russo *et al.*, 1996) and the Src-family tyrosine kinase

LCK (Yamaguchi and Hendrickson, 1996). A comparison with these kinase structures reveals that pTyr1163 in the IRK A-loop is structurally related to phosphothreonine (pThr)197 in cAPK, pThr160 in CDK2 and pTyr394 in LCK (Figure 4B–D).

Although pTyr1163 is in a spatial position similar to pThr197/pThr160 in cAPK/CDK2, the number of hydrogen-bonding interactions in which pTyr1163 participates is far fewer than for the pThr residues (Figure 4B
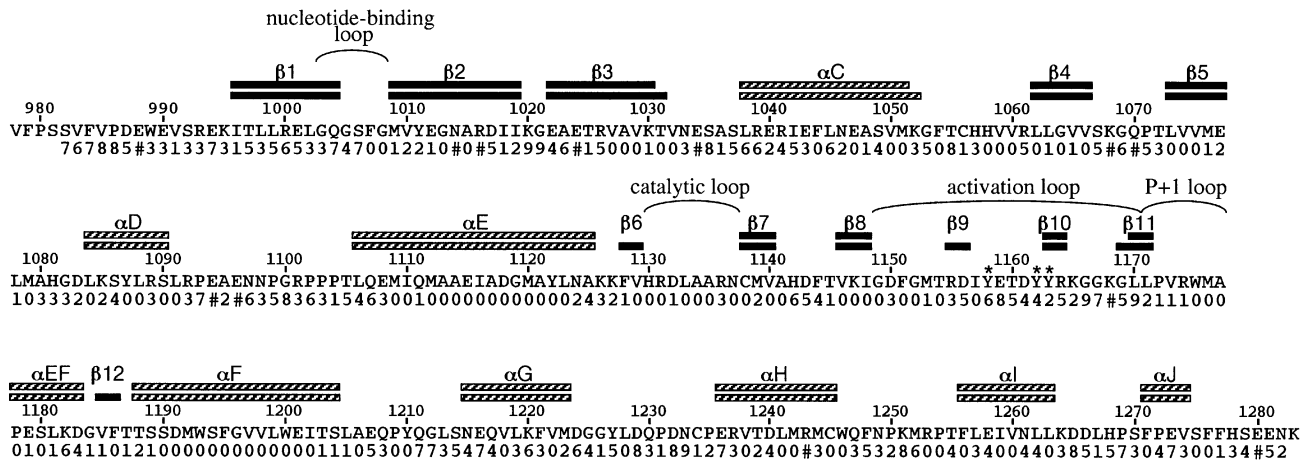
nucleotide-binding
loop

β1    β2    β3    αC    β4    β5

980    990    1000    1010    1020    1030    1040    1050    1060    1070
VFPSSVFVPDEWEVSREKITLLRELGQGSFGMVYEGNARDIIKGEAETRVAVKTVNESASLRERIEFLNEASVMKGFTCHHVVRLLGVVSKGQPTLVVME
767885#331337315356533747001221 0#0#5129946#150001003#8156624530620140035081300050 10105#6#5300012

catalytic loop    activation loop    P+1 loop

αD    αE    β6    β7    β8    β9    β10    β11

1080    1090    1100    1110    1120    1130    1140    1150    1160    1170
LMAHGDLKSYLRSLRPEAENNPGRPPPPTLQEMIQMAAEIADGMAYLNAKKFVHRDLAARNCMVAHDFTVKIGDFGMTRDIYETDYYRKGGKGLLPVRWMA
1033320240030037#2#65836315463001000000000000024321000100030020065410000300103506854425297#592111000

αEF  β12    αF    αG    αH    αI    αJ

1180    1190    1200    1210    1220    1230    1240    1250    1260    1270    1280
PESLKDGVFTTSSDMWSFGVVLWEITSLAEQPYQGLSNEQVLKFVMDGGYLDQPDNCPERVTDLMRMCWQFNPKMRPTFLEIVNLLKDDLHPSFPEVSFFHSEENK
010164110121000000000000001110530077354740363026415083189127302400#300353286004034004403851573047300134#52

**Fig. 3.** Secondary structure comparison of IRK and IRK3P and residue solvent accessibility. The secondary structure assignments for IRK and IRK3P were obtained using PROCHECK (Laskowski *et al.*, 1993). Striped bars delineate α-helices and black bars delineate β-strands. The assignments for IRK appear on top and those for IRK3P on bottom. The three autophosphorylation sites in the activation loop are marked with an asterisk. The numbers under the amino acid sequence represent the fractional solvent accessibility (FSA) of the residue in the IRK3P structure. The FSA is the ratio of the solvent-accessible surface area of a residue in a GXG tri-peptide to that in the IRK3P structure. A value of 0 represents an FSA between 0.00 and 0.09, 1 represents an FSA between 0.10 and 0.19, etc. The higher the FSA, the more solvent-exposed the residue. The FSAs were computed in the absence of MgAMP-PNP, peptide substrate and water molecules. A # in the FSA line indicates that the side chain for that residue is not included in the atomic model due to disorder.

and C). Arg1131, the residue which immediately precedes the putative catalytic base, Asp1132, is highly conserved in both the tyrosine and serine/threonine kinase families. In the cAPK and CDK2 structures (Knighton *et al.*, 1991; Russo *et al.*, 1996), the corresponding arginine is directly hydrogen-bonded to the pThr. Arg1131, however, is not observed to interact directly with pTyr1163. In the LCK structure, pTyr394 is also engaged in relatively few interactions, differing somewhat from those seen for pTyr1163 (Figure 4D), which suggests a susceptibility of these pTyr residues to the action of tyrosine phosphatases (Yamaguchi and Hendrickson, 1996).

A comparison of the phosphorylated A-loops of IRK3P and LCK (one residue shorter) shows that the conformation is similar at the beginning of the loop, which includes the conserved [1150]DFG residues ([382]DFG), but diverges after pTyr1163 (pTyr394) (Figure 4B and D). Residues at the end of the LCK A-loop, including kinase-conserved Pro403 (Pro1172), are displaced further from the active site than the corresponding residues in IRK3P. Interestingly, based on the mode of peptide substrate binding observed in the present structure (discussed below), the C-terminal end of the A-loop in the unliganded LCK structure is not properly positioned for peptide binding.

### Lobe closure

The rearrangement of the insulin receptor A-loop upon autophosphorylation facilitates a reorientation of the N- and C-terminal lobes of the kinase, which is necessary for productive ATP binding. In the structure of the unphosphorylated kinase domain of the FGF receptor, the ATP binding site is accessible, yet full engagement of ATP by the kinase does not occur due to interactions that impede lobe rotation (Mohammadi *et al.*, 1996b). In the IRK structure, the lobes are held apart by steric interactions between residues of the nucleotide-binding loop (1003–1008) and the [1150]DFG residues. When the C-terminal lobes of IRK and ternary IRK3P are superimposed, a nearly pure rotation of the N-terminal lobe of IRK by

~21° aligns the five-stranded β-sheets (Figure 2B). The direction of the rotation is both towards the C-terminal lobe and parallel to the long axis of the molecule. Three pivot points in the rotation can be identified: two in the loop between αC and β4 (near Phe1054 and Arg1061) and one near the last residue of β5 (Glu1077), just before the segment connecting the two lobes (between β5 and αD). The protein kinase-conserved glycine in the connecting segment, Gly1082, does not appear to play a role in facilitating lobe movement.

With respect to cAPK, the only other protein kinase for which structures of a ternary complex (with nucleotide and peptide) have been reported (Bossemeyer *et al.*, 1993; Zheng *et al.*, 1993), the lobes of IRK3P are rotated by ~17°. Despite this difference, the actual lobe separation in the IRK3P and cAPK structures is similar as measured by the Cα–Cα distance between Val1010 (Val57) and Met1139 (Leu173), which flank the ATP adenine. This distance is 12.8 Å in ternary IRK3P (15.0 Å in IRK) and 12.9 Å in ternary cAPK. The lobe configuration in unliganded LCK (Yamaguchi and Hendrickson, 1996) is ~8° more open than that in ternary IRK3P, with a corresponding lobe–lobe separation of 13.9 Å.

Upon lobe closure, the β-sheet in the N-terminal lobe of IRK3P moves approximately as a rigid body. However, αC rotates an additional ~35° towards the C-terminal lobe (Figure 2C). This movement of αC places protein kinase-conserved Glu1047 in proximity (4.4 Å) to conserved Lys1030 in the ATP binding site. Three hydrophobic residues which lie along the same face of αC, Leu1038, Ile1042 and Leu1045, are solvent-exposed in the IRK3P structure, whereas the latter two residues are partially buried in the IRK structure (Figure 2C). These hydrophobic residues, which are not conserved in the tyrosine kinase family, are perhaps involved in protein–protein interactions specific to insulin receptor subfamily members.

### MgAMP-PNP binding

The entire AMP-PNP molecule is well ordered in the ternary IRK3P structure (Figure 1), indicative of a pro-
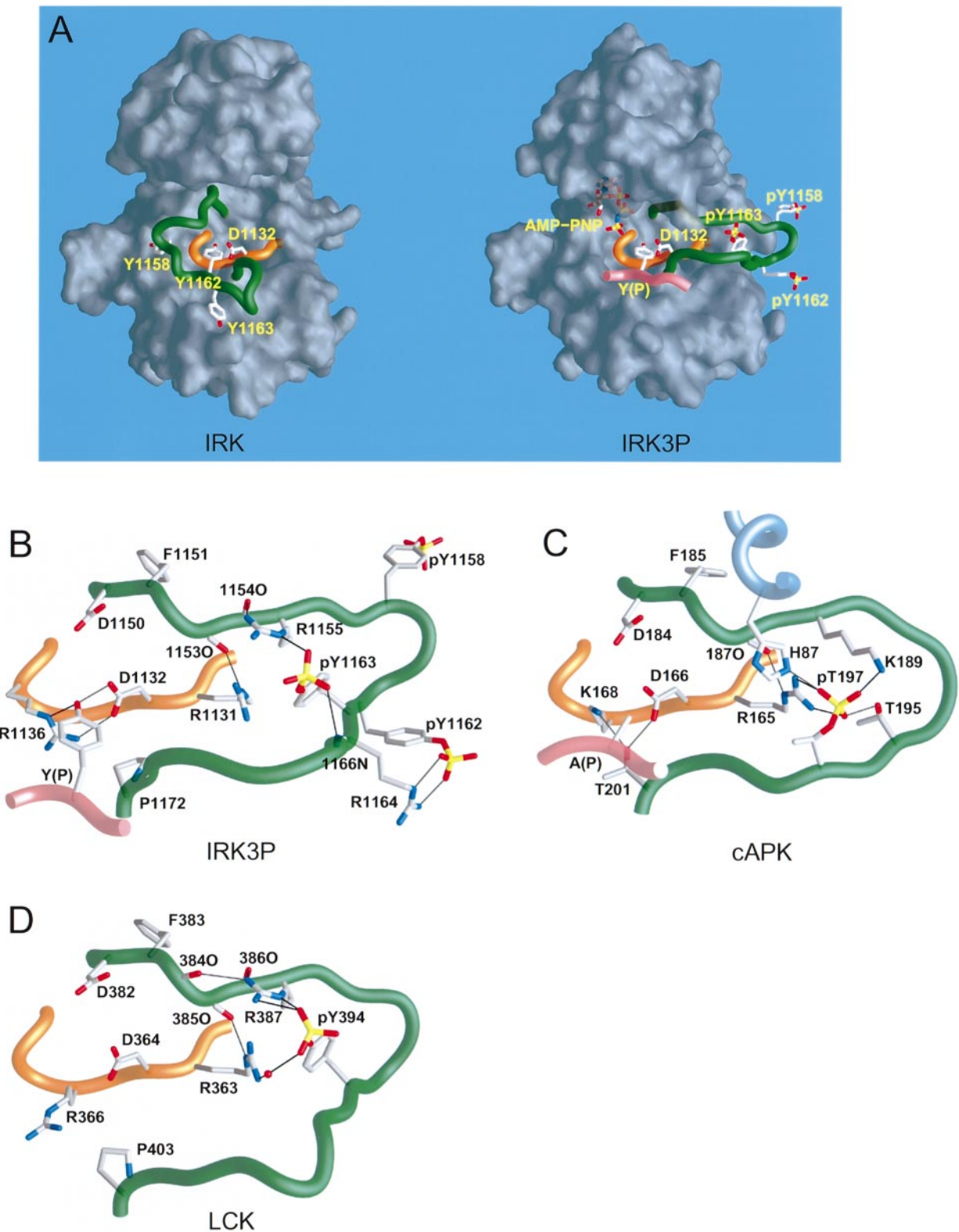
**Fig. 4.** Conformation of the IRK3P A-loop and comparison with other kinase A-loops. (**A**) Comparison of the A-loop conformations in IRK and IRK3P. The activation loop is colored green, the catalytic loop orange and the peptide substrate pink. The rest of the protein in each case is represented by a semi-transparent molecular surface. Also shown is AMP-PNP, which is partially masked by the N-terminal lobe of IRK3P. Carbon atoms are colored white, nitrogen atoms blue, oxygen atoms red and phosphorus atoms yellow. View is ~90° from that in Figure 2A, from the right side. (**B**) Selected hydrogen-bonding interactions for activation loop residues of IRK3P are shown as black lines. Atom coloring is the same as in (A) except that carbon atoms are gray. Coloring of the backbone representation is the same as in (A). Only a portion of the peptide substrate backbone is shown (P–1 to P+1). (**C**) Selected hydrogen-bonding interactions for activation loop residues of cAPK (Zheng *et al.*, 1993) are shown as black lines. Coloring same as in (B), with other backbone segments colored blue. Only a portion of the peptide inhibitor backbone is shown (P–1 to P+1). (**D**) Selected hydrogen-bonding interactions for activation loop residues of LCK (Yamaguchi and Hendrickson, 1996) are shown as black lines. Coloring same as in (B). Figure prepared with GRASP (Nicholls *et al.*, 1991).
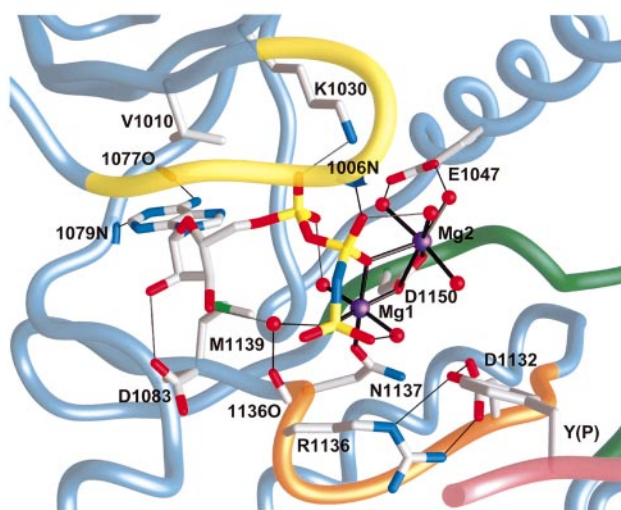
**Fig. 5.** Interactions of MgAMP-PNP in the ternary IRK3P structure. The coloring of the backbone representation is the same as in Figure 4B, with the nucleotide-binding loop colored yellow. Atom coloring is the same as in Figure 4B, with sulfur atoms colored green and $Mg^{2+}$ ions colored purple. Selected hydrogen bonds are shown as thin black lines and bonds to $Mg^{2+}$ ions are shown as thick black lines. Figure prepared with GRASP (Nicholls *et al.*, 1991).

ductive binding mode. The interactions of AMP-PNP with IRK3P are illustrated in Figure 5. The adenine is situated between Val1010 and Met1139, and hydrogen-bonded to backbone groups of Glu1077 and Met1079. One of the ribose hydroxyl groups (O2′) is hydrogen-bonded to the side chain of Asp1083, and the other (O3′) is hydrogen-bonded via a water molecule to the carbonyl oxygen of Arg1136 in the catalytic loop. The analogous interactions for the adenine and ribose are observed in the ternary cAPK structure (Bossemeyer *et al.*, 1993; Zheng *et al.*, 1993), except that O3′ is hydrogen-bonded directly to the carbonyl oxygen of Glu170 (Arg1136).

The interactions of the nucleotide phosphate groups with IRK3P residues differ from those observed in the ternary cAPK structure. In cAPK, the nucleotide-binding loop is hydrogen-bonded via three backbone groups to the β- and γ-phosphates of ATP (Bossemeyer *et al.*, 1993; Zheng *et al.*, 1993). In IRK3P, only one hydrogen bond is observed, between the backbone amide nitrogen of Ser1006 and the β-phosphate (Figure 5). Moreover, in cAPK, protein kinase-conserved Lys72 is hydrogen-bonded to the α- and β-phosphates, whereas in IRK3P, Lys1030 is hydrogen-bonded to just the α-phosphate.

The greater extension of the nucleotide-binding loop over the phosphates in ternary cAPK is probably due to hydrogen-bonding between the loop and the peptide inhibitor PKI (Bossemeyer *et al.*, 1993). In the ternary IRK3P structure, no interactions are observed between the nucleotide-binding loop and the peptide substrate. Owing to the longer side chain of tyrosine versus serine/threonine, the peptide substrate is positioned significantly further away from the N-terminal lobe in IRK3P than in cAPK (Figure 4B and C). It is likely, therefore, that the lack of interaction with the nucleotide-binding loop is a general feature of protein substrate–tyrosine kinase interactions.

Two well-ordered $Mg^{2+}$ ions have been included in the

atomic model based on the heights of the electron density peaks and the number and distances of coordinating atoms (Figures 1 and 5). Mg1 shows nearly ideal octahedral coordination by six oxygen atoms (Mg⋯O = 2.0–2.2 Å): one from each of the β- and γ-phosphates, one from each of the side chains of protein kinase-conserved Asn1137 (catalytic loop) and Asp1150 (A-loop), and two from well-ordered water molecules (Figure 5). Mg2 has seven oxygen ligands (Mg⋯O = 2.4–2.6 Å): the same β-phosphate oxygen that coordinates Mg1, both carboxylate oxygens of Asp1150, and four water molecules. Mg1 and Mg2 are in positions similar to those of the inhibitory and activating metal ions, respectively, in ternary cAPK (Bossemeyer *et al.*, 1993; Zheng *et al.*, 1993), but the coordination by the phosphate groups differs. Mg1 is coordinated by the β- and γ-phosphates, whereas the inhibitory metal ion in ternary cAPK is coordinated by the α- and γ-phosphates. Mg2 is coordinated by just the β-phosphate, whereas the activating metal ion in ternary cAPK is coordinated by the β- and γ-phosphates. The coordination environment of Mg1 is strikingly similar to that of the $Mg^{2+}$ ion in the structures of GTPases such as Ras (with MgGMP-PNP; Pai *et al.*, 1990) and transducin-α (with MgGTPγS; Noel *et al.*, 1993), wherein the $Mg^{2+}$ ion is octahedrally coordinated by the β- and γ-phosphates, two side-chain oxygens, and two water molecules, in the same spatial configuration as found in the ternary IRK3P structure.

### Peptide substrate binding

The 18-residue peptide substrate that was co-crystallized with IRK3P and MgAMP-PNP was derived from a putative insulin receptor phosphorylation site on rat IRS-1, Tyr727 (Sun *et al.*, 1991). This peptide, KKKLPATGDYMN-MSPVGD, has a reported $K_m$ of 24 μM (Shoelson *et al.*, 1992). Of the 18 residues, supporting electron density is seen for only six, from the P–2 to the P+3 residue [GDYMNM; P-residue is the acceptor tyrosine, Tyr(P)]. The residues C-terminal to Tyr(P) form a short β-strand which pairs in an anti-parallel manner with residues of β11 at the end of the A-loop (Figures 2A and 6B). Backbone hydrogen-bonding is observed between Met(P+1) and Leu1171, and between Met(P+3) and Gly1169.

Tyrosine residues in YMXM motifs are efficient substrates of the insulin receptor *in vitro* and *in vivo* (Shoelson *et al.*, 1992; Sun *et al.*, 1993; Songyang *et al.*, 1995). In the ternary IRK3P structure, the methionine side chains of the peptide fit into two adjacent hydrophobic pockets on the surface of the C-terminal lobe, composed of residues from the P+1 loop (1171–1176) and from αEF and αG (Figure 6). The pocket for Met(P+1) comprises Val1173, Leu1219 and the aliphatic portions of the Asn1215 and Glu1216 side chains. The pocket for Met(P+3) comprises Leu1171, Val1173, Met1176, Leu1181 and Leu1219. These pockets appear to be optimized for accommodating long hydrophobic side chains.

The ternary IRK3P structure provides a basis for understanding tyrosine kinase substrate specificity. In a study of substrate specificity using a degenerate peptide library, the cytoplasmic tyrosine kinase Fps was shown to have a strong preference for glutamic acid at the P+1 position of a peptide substrate (Songyang *et al.*, 1995). Of the four insulin receptor residues that form the binding pocket for
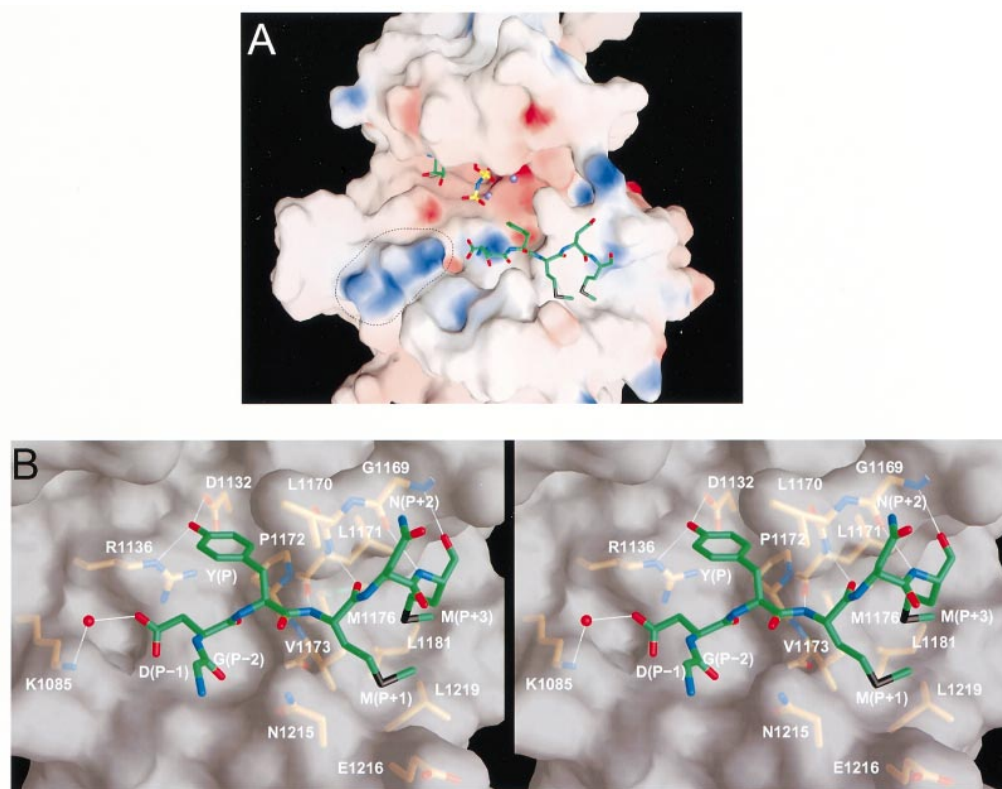
**Fig. 6.** Mode of peptide substrate binding. (**A**) Overall view of peptide substrate binding to IRK3P. The molecular surface of IRK3P is colored according to electrostatic potential (calculated in the absence of MgAMP-PNP and peptide). Positive potential is shown in blue, negative potential in red and neutral potential in white. Carbon atoms are green, oxygen atoms are red, nitrogen atoms are blue, sulfur atoms are black and phosphorus atoms are yellow. The dotted line encompasses Lys1085, Arg1089 and Arg1092 of αD. View is approximately the same as in Figure 4A. (**B**) Stereo view of the interactions between the peptide substrate and IRK3P. Oxygen atoms are red, nitrogen atoms are blue, carbon atoms of IRK3P/peptide are orange/green and sulfur atoms of IRK3P/peptide are green/black. The molecular surface is semi-transparent, and selected hydrogen bonds are shown as white lines. The red sphere represents a water molecule. Figure prepared with GRASP (Nicholls *et al.*, 1991).

Met(P+1), three are identical or similar in Fps, while the fourth, Leu1219, is an arginine in Fps (Arg770). Modeling suggests that an arginine at the Leu1219 position could make a hydrogen bond with a glutamic acid at the P+1 position of a peptide substrate. In the receptor tyrosine kinase RET, the substitution Met918→Thr leads to multiple endocrine neoplasia type 2B (Hofstra *et al.*, 1994), and is thought to alter the substrate specificity of RET (Songyang *et al.*, 1995; Pandit *et al.*, 1996). The corresponding methionine in the insulin receptor, Met1176, is a constituent of the Met(P+3) binding pocket.

Substrates of the insulin receptor and other tyrosine kinases often contain one or more acidic residues N-terminal to the acceptor tyrosine (Hunter, 1982; Stadtmauer and Rosen, 1983; Songyang *et al.*, 1995). The co-crystallized peptide contains an aspartic acid at the P–1 position. In the crystal structure, Asp(P–1) is not directly hydrogen-bonded to residues of the kinase, but instead makes a water-mediated hydrogen bond to Lys1085 (Figure 6B). Two other positively charged residues, Arg1089 and Arg1092, extend from the same face of αD as Lys1085 towards the substrate binding region (Figure 6A). At the position corresponding to Arg1089, a large majority of tyrosine kinases contain a hydrogen-bond donor which is often positively charged. This residue may play a role in the recognition of protein substrates with acidic residues at the P–3 or P–4 position.

### Active site

The hydroxyl group of the substrate tyrosine, Tyr(P), is hydrogen-bonded to the carboxylate group of Asp1132 (Oη⋯Oδ2 = 2.7 Å), and thus appears to be in position for proton abstraction by Asp1132 (Figures 4B and 5). The hydroxyl group is also hydrogen-bonded to tyrosine kinase-conserved Arg1136 in the catalytic loop (Oη⋯Nε = 3.1 Å). The phenolic ring of Tyr(P) is oriented in part by van der Waals interactions with tyrosine kinase-conserved Pro1172 (P+1 loop), positioned 3.6 Å from the ring (Figures 4B and 6B).

Based on the autoinhibited IRK structure, a difference in the conformation of the P+1 loop near Pro1172 appeared to be a major determinant in conferring specificity for tyrosine versus serine/threonine (Hubbard *et al.*, 1994; Taylor *et al.*, 1995). This is confirmed by the ternary IRK3P structure, in which backbone hydrogen-bonding between the peptide substrate and the P+1 loop of the kinase governs the distance between the peptide backbone and the kinase active site (Figure 6B); the side chain of tyrosine but not of serine/threonine is long enough to reach the active site.

In the ternary IRK3P structure, the γ-phosphorus atom of AMP-PNP is 5.0 Å from the hydroxyl oxygen of Tyr(P) (Figure 5), and is therefore not in position for direct in-line (associative) phosphotransfer, the catalytic mechanism proposed for cAPK (Madhusudan *et al.*, 1994). The use

of AMP-PNP in co-crystallizations (to preclude substrate phosphorylation) could introduce a deviation in γ-phosphate positioning, although no significant differences in nucleotide binding are seen in the structures of cAPK with ATP (Zheng *et al.*, 1993) or with AMP-PNP (Bossemeyer *et al.*, 1993). The present structure is the first to be reported of a complex between a protein kinase, a peptide substrate, and a γ-phosphate-containing nucleotide. Trapping the enzyme with both the non-transferable γ-phosphate and acceptor hydroxyl in position for associative phosphotransfer may be inherently difficult. Alternatively, in view of the difference in the p*K*a values of tyrosine (~10) and serine/threonine (~13), and the presence in the catalytic loop of an arginine (tyrosine kinases) rather than a lysine (serine/threonine kinases), the structure may suggest a dissociative or mixed associative–dissociative phosphotransfer mechanism (Bramson *et al.*, 1984) for tyrosine kinases.

### Functional implications

The crystal structures of IRK and IRK3P afford an understanding at the molecular level of insulin receptor activation via autophosphorylation. The IRK structure, together with mutagenesis data showing that substitution of Tyr1162 with phenylalanine increases basal level kinase activity (Ellis *et al.*, 1986), suggests that residues of the unphosphorylated A-loop compete with ATP and protein substrates for binding at the kinase active site. Upon insulin-triggered *trans*-autophosphorylation of the tyrosine residues within the A-loop, this peptide segment adopts a markedly different conformation which is stabilized by both pTyr and non-pTyr interactions. For the insulin receptor and presumably other receptor tyrosine kinases, stimulation of kinase activity by autophosphorylation is evidently a consequence of stabilization of an A-loop conformation that (i) allows unhindered access to ATP and protein substrates, and (ii) facilitates the correct positioning of the residues critical for MgATP binding and catalysis.

The bridging interactions of pTyr1163 with other A-loop residues and its similar spatial position to pThr197 in cAPK imply that pTyr1163 is the key pTyr in stabilizing the conformation of the tris-phosphorylated A-loop. Although studies of Tyr→Phe substitutions in the insulin receptor A-loop have not demonstrated a predominant role in kinase activation for a particular tyrosine (Tavare and Siddle, 1993), the tyrosine corresponding to Tyr1163 has been shown to be the critical autophosphorylation site in the FGF receptor (Mohammadi *et al.*, 1996a) and in MET (Longati *et al.*, 1994).

Autophosphorylation mapping experiments have indicated that Tyr1163 is the last of the three A-loop sites to be phosphorylated (Dickens and Tavare, 1992; Wei *et al.*, 1995). This result, together with the mutagenesis data and the structural results presented here, is consistent with a graded activation mechanism in which each autophosphorylation event in the A-loop leads to partial stabilization of the active configuration of the A-loop, with full activation achieved only upon autophosphorylation of pTyr1163. Conceivably, in partially activated (mono- and bis-phosphorylated) states, pTyr1158 and pTyr1162 are engaged in a different set of interactions than those observed in the IRK3P structure. For example, pTyr1162 may substitute

structurally for pTyr1163 in the bis-phosphorylated state, though presumably less effectively.

The lack of engagement of pTyr1158 with other kinase residues and the solvent accessibility of the pTyr1162/Arg1164 pair suggests that these pTyr residues could potentially serve as docking sites for downstream signaling proteins. Several recent studies have provided evidence that one or more of the A-loop pTyr residues are involved in protein–protein interactions. Yeast two-hybrid experiments have identified an interaction between a region in IRS-2 and the cytoplasmic domain of the insulin receptor, which is dependent on tyrosine phosphorylation in the A-loop but not in the juxtamembrane region or C-terminal tail (He *et al.*, 1996; Sawka-Verhelle *et al.*, 1996). Other yeast two-hybrid experiments together with *in vitro* binding studies have provided evidence for interactions between the cytoplasmic domain and the Src-homology 2 (SH2) domains of GRB10/IR-SV1 (O'Neill *et al.*, 1996; Frantz *et al.*, 1997) and SHP-2 (Kharitonenkov *et al.*, 1995), which are dependent on phosphorylation of one or more of the A-loop tyrosine residues. The IRK3P structure provides evidence, albeit circumstantial, that one or more pTyr residues of the insulin receptor A-loop may serve as targets for downstream signaling molecules.

## Materials and methods

### Expression, purification and crystallization of IRK3P

A recombinant baculovirus was engineered to encode residues 978–1283 of the human insulin receptor with the inclusion of two amino acid substitutions: Cys981→Ala and Tyr984→Phe (Wei *et al.*, 1995). Expression and purification of IRK have been described previously (Hubbard *et al.*, 1994). Typically, IRK3P was produced by adding ATP and MgCl$_2$ (10 mM and 25 mM final, respectively) to IRK (~1 mg/ml final) at 4°C. After 20–30 min, the autophosphorylation reaction was terminated by the addition of EDTA (50 mM final). The reaction mixture was passed over a Superdex 75 (Pharmacia) gel filtration column to remove nucleotides, Mg$^{2+}$ and EDTA. The mainly tris-phosphorylated kinase species was separated from the bis-phosphorylated species by Mono Q (Pharmacia) ion exchange chromatography. Purified IRK3P was concentrated to 10–15 mg/ml using a Centricon-10 (Amicon) in 20 mM Tris–HCl, pH 7.5, 200 mM NaCl and 200 μM Na$_3$VO$_4$. Solid-phase synthesis of the 18-residue peptide substrate was performed on an Applied Biosystems model 741A synthesizer using Fmoc chemistry, and AMP-PNP was purchased from Boehringer-Mannheim.

Crystals were grown at 4°C by vapor diffusion in hanging drops containing 2.0 μl of protein solution (10 mg/ml IRK3P, 2 mM AMP-PNP, 6 mM MgCl$_2$ and 0.5 mM peptide substrate) and 2.0 μl of reservoir solution [22% polyethylene glycol (PEG) 8000, 100 mM Tris–HCl, pH 7.5, and 2% ethylene glycol]. The crystals belong to trigonal space group P3$_2$21 and have unit cell dimensions of $a = b = 66.5$ Å, $c = 139.1$ Å when frozen. There is one molecule in the asymmetric unit and the solvent content is 50% (assuming a partial specific volume of 0.74 cm$^3$/g).

### Data collection, structure determination and analysis

One cryo-cooled crystal was used for data collection. The crystal was transferred into a cryo-protectant containing 25% PEG 8000, 1 mM AMP-PNP, 3 mM MgCl$_2$, 0.25 mM peptide substrate, 100 mM Tris–HCl, pH 7.5 and 15% ethylene glycol. After ~1 min in the cryo-protectant, the crystal was flash-cooled in liquid nitrogen and then transferred to the goniostat, which was bathed in a dry nitrogen stream at –160°C. Data were collected at beamline X4A at the National Synchrotron Light Source, Brookhaven National Laboratory, on Fuji image plates and digitized with a Fuji scanner. All data were processed using DENZO and SCALEPACK (Otwinowski, 1993).

A molecular replacement solution was found with a search molecule consisting of IRK residues 981–1283, excluding 1149–1170 (A-loop), for which the N-terminal lobe (residues 981–1081) was rotated and translated as a rigid body so that the relative orientation of the N- and

C-terminal lobes was similar to that in closed-form cAPK (Zheng *et al.*, 1993). An initial 3.0 Å data set collected on a Rigaku R-AXIS IIC image plate detector was used for molecular replacement (data not shown). With AMoRe (Navaza, 1994), using 80% of the structure factor amplitudes between 15.0 and 3.5 Å, the correlation coefficient for the correct solution in space group $P3_221$ was 0.46 versus 0.34 for the highest incorrect solution in the enantiomeric space group $P3_121$. The AMoRe solution was refined in X-PLOR (Brünger, 1992), first as one rigid-body unit, then as two units each comprising a lobe of the kinase (981–1081, 1082–1283), resulting in a relative rotation of the two lobes of ~13° and an increase of the correlation coefficient from 0.33 to 0.41 (10.0–3.4 Å, F>2σ). Simulated annealing and conjugate-gradient minimization were performed using X-PLOR, and model building was performed using TOM/FRODO (Jones, 1985).

The average atomic B-factors are 18.5 Å$^2$ for protein, 15.8 Å$^2$ for MgAMP-PNP, 21.9 Å$^2$ for peptide and 25.3 Å$^2$ for water molecules. Due to poor supporting electron density, residues 978–980 are not included in the atomic model, nor are the side chains indicated in Figure 3. Atomic superpositions were performed with TOSS (Hendrickson, 1979). Per residue solvent accessible surface calculations were done with X-PLOR with a probe radius of 1.4 Å. As defined in PROCHECK (Laskowski *et al.*, 1993), the backbone torsion angles of the protein lie either in most favored regions (93%) or in additional allowed regions (7%).

## Acknowledgements

## References

Bossemeyer,D., Engh,R.A., Kinzel,V., Ponstingl,H. and Huber,R. (1993) Phosphotransferase and substrate binding mechanism of the cAMP-dependent protein kinase catalytic subunit from porcine heart as deduced from the 2.0 Å structure of the complex with $Mn^{2+}$ adenylyl imidodiphosphate and inhibitor peptide PKI(5–24). *EMBO J.*, **12**, 849–859.

Bramson,H.N., Kaiser,E.T. and Mildvan,A.S. (1984) Mechanistic studies of cAMP-dependent protein kinase action. *CRC Crit. Rev. Biochem.*, **15**, 93–123.

Brünger,A.T. (1992) X-PLOR (Version 3.1) Manual (New Haven, CT: The Howard Hughes Medical Institute and Department of Molecular Biophysics and Biochemistry, Yale University).

Carson,M. (1991) Ribbons 2.0. *J. Appl. Crystallogr.*, **24**, 958–961.

Dickens,M. and Tavare,J.M. (1992) Analysis of the order of autophosphorylation of human insulin receptor tyrosines 1158, 1162 and 1163. *Biochem. Biophys. Res. Commun.*, **186**, 244–250.

Ebina,Y. *et al.* (1985) The human insulin receptor cDNA: the structural basis for hormone-activated transmembrane signalling. *Cell*, **40**, 747–758.

Ellis,L., Clauser,E., Morgan,D.O., Edery,M., Roth,R.A. and Rutter,W.J. (1986) Replacement of insulin receptor tyrosine residues 1162 and 1163 compromises insulin-stimulated kinase activity and uptake of 2-deoxyglucose. *Cell*, **45**, 721–732.

Evans,S.V. (1993) SETOR: hardware lighted three-dimensional solid model representations of macromolecules. *J. Mol. Graphics*, **11**, 134–138.

Feener,E.P., Backer,J.M., King,G.L., Wilden,P.A., Sun,X.J., Kahn,C.R. and White,M.F. (1993) Insulin stimulates serine and tyrosine phosphorylation in the juxtamembrane region of the insulin receptor. *J. Biol. Chem.*, **268**, 11256–11264.

Frantz,J.D., Giorgett-Peraldi,S., Ottinger,E.A. and Shoelson,S.E. (1997) Human GRB-IRβ/GRB10. Splice variants of an insulin and growth factor receptor-binding protein with PH and SH2 domains. *J. Biol. Chem.*, **272**, 2659–2667.

Hanks,S.K., Quinn,A.M. and Hunter,T. (1991) The protein kinase family: conserved features and deduced phylogeny of the catalytic domains. *Science*, **241**, 42–52.

He,W., Craparo,A., Zhu,Y., O'Neill,T.J., Wang,L.-M., Pierce,J. and Gustafson,T.A. (1996) Interaction of insulin receptor substrate-2 (IRS-2) with the insulin and insulin-like growth factor I receptors. *J. Biol. Chem.*, **271**, 11641–11645.

Hendrickson,W.A. (1979) Transformations to optimize the superposition of similar structures. *Acta Crystallogr.*, **A35**, 158–163.

Hofstra,R.M. *et al.* (1994) A mutation in the RET proto-oncogene associated with multiple endocrine neoplasia type 2B and sporadic medullary thyroid carcinoma. *Nature*, **367**, 375–376.

Hubbard,S.R., Wei,L., Ellis, L. and Hendrickson,W.A. (1994) Crystal structure of the tyrosine kinase domain of the human insulin receptor. *Nature*, **372**, 746–754.

Hunter,T. (1982) Synthetic peptide substrates for a tyrosine protein kinase. *J. Biol. Chem.*, **257**, 4843–4848.

Jones,T.A. (1985) Diffraction methods for biological macromolecules. Interactive computer graphics: FRODO. *Methods Enzymol.*, **115**, 157–171.

Kato,H., Faria,T.N., Stannard,B., Roberts,C.T. and LeRoith,D. (1994) Essential role of tyrosine residues 1131, 1135, and 1136 of the insulin-like growth factor-I (IGF-I) receptor in IGF-I action. *Mol. Endocrinol.*, **8**, 40–50.

Kharitonenkov,A., Schnekenburger,J., Chen,Z., Knyazev,P., Ali,S., Zwick,E., White,M. and Ullrich,A. (1995) Adapter function of protein-tyrosine phosphatase 1D in insulin receptor/insulin receptor substrate-1 interaction. *J. Biol. Chem.*, **270**, 29189–29193.

Knighton,D.R., Zheng,J., Ten Eyck,L.F., Ashford,V.A., Xuong,N.H., Taylor,S.S. and Sowadski,J.M. (1991) Crystal structure of the catalytic subunit of cyclic adenosine monophosphate-dependent protein kinase. *Science*, **253**, 407–414.

Kohanski,R.A. (1993) Insulin receptor autophosphorylation. II. Determination of autophosphorylation sites by chemical sequence analysis and identification of the juxtamembrane sites. *Biochemistry*, **32**, 5773–5780.

Laskowski,R.A., MacArthur,M.W., Moss,D.S. and Thornton,J.M. (1993) PROCHECK: a program to check the stereochemical quality of protein structures. *J. Appl. Crystallogr.*, **26**, 283–291.

Longati,P., Bardelli,A., Ponzetto,C., Naldini,L. and Comoglio,P.M. (1994) Tyrosines 1234–1235 are critical for activation of the tyrosine kinase encoded by the MET proto-oncogene (HGF receptor). *Oncogene*, **9**, 49–57.

Madhusudan, Trafny,E.A., Xuong,N.H., Adams,J.A., Ten Eyck,L.F., Taylor,S.S. and Sowadski,J.M. (1994) cAMP-dependent protein kinase: crystallographic insights into substrate recognition and phospho-transfer. *Protein Sci.*, **3**, 176–187.

Middlemas,D.S., Meisenhelder,J. and Hunter,T. (1994) Identification of TrkB autophosphorylation sites and evidence that phospholipase C-γ1 is a substrate of the TrkB receptor. *J. Biol. Chem.*, **269**, 5458–5466.

Mitra,G. (1991) Mutational analysis of conserved residues in the tyrosine kinase domain of the human trk oncogene. *Oncogene*, **6**, 2237–2241.

Mohammadi,M., Dikic,I., Sorokin,A., Burgess,W.H., Jaye,M. and Schlessinger,J. (1996a) Identification of six novel autophosphorylation sites on fibroblast growth factor receptor 1 and elucidation of their importance in receptor activation and signal transduction. *Mol. Cell. Biol.*, **16**, 977–989.

Mohammadi,M., Schlessinger,J. and Hubbard,S.R. (1996b) Structure of the FGF receptor tyrosine kinase domain reveals a novel autoinhibitory mechanism. *Cell*, **86**, 577–587.

Navaza,J. (1994) AMoRe: an automated package for molecular replacement. *Acta Crystallogr.*, **A50**, 157–163.

Nicholls,A., Sharp,K.A. and Honig,B. (1991) Protein folding and association: insights from the interfacial and thermodynamic properties of hydrocarbons. *Proteins*, **11**, 281–296.

Noel,J.P., Hamm,H.E. and Sigler,P.B. (1993) The 2.2 Å crystal structure of transducin-α complexed with GTPγS. *Nature*, **366**, 654–663.

O'Neill,T.J., Rose,D.W., Pillay,T.S., Hotta,K., Olefsky,J.M. and Gustafson,T.A. (1996) Interaction of a GRB-IR splice variant (a human GRB10 homolog) with the insulin and insulin-like growth factor I receptors. Evidence for a role in mitogenic signaling. *J. Biol. Chem.*, **271**, 22506–22513.

Otwinowski,Z. (1993) Oscillation data reduction program. In Sawyer,L., Isaacs,N. and Bailey,S. (eds), *Proceedings of the CCP4 Study Weekend*. SERC Daresbury Laboratory, Daresbury, UK, pp. 56–62.

Pai,E.F., Krengel,U., Petsko,G.A., Goody,R.S., Kabsch,W. and Wittinghofer,A. (1990) Refined crystal structure of the triphosphate conformation of H-ras p21 at 1.35 Å resolution: implications for the mechanism of GTP hydrolysis. *EMBO J.*, **9**, 2351–2359.

Pandit,S.D., Donis-Keller,H., Iwamoto,T., Tomich,J.M. and Pike,L.J. (1996) The multiple endocrine neoplasia type 2B point mutation alters long-term regulation and enhances the transforming capacity of the epidermal growth factor receptor. *J. Biol. Chem.*, **271**, 5850–5858.

Rosen,O.M., Herrera,R., Olowe,Y., Petruzzelli,L.M. and Cobb,M.H. (1983) Phosphorylation activates the insulin receptor tyrosine protein kinase. *Proc. Natl Acad. Sci. USA*, **80**, 3237–3240.

Russo,A.A., Jeffrey,P.D. and Pavletich,N.P. (1996) Structural basis of cyclin-dependent kinase activation by phosphorylation. *Nature Struct. Biol.*, **3**, 696–700.

Sawka-Verhelle,D., Tartare-Deckert,S., White,M.F. and Van Obberghen,E. (1996) Insulin receptor substrate-2 binds to the insulin receptor through its phosphotyrosine-binding domain and through a newly identified domain comprising amino acids 591–786. *J. Biol. Chem.*, **271**, 5980–5983.

Shoelson,S.E., Chatterjee,S., Chaudhuri,M. and White,M.F. (1992) YMXM motifs of IRS-1 define substrate specificity of the insulin receptor kinase. *Proc. Natl Acad. Sci. USA*, **89**, 2027–2031.

Songyang,Z. *et al*. (1995). Catalytic specificity of protein-tyrosine kinases is critical for selective signalling. *Nature*, **373**, 536–539.

Stadtmauer,L.A. and Rosen,O.M. (1983) Phosphorylation of exogenous substrates by the insulin receptor-associated protein kinase. *J. Biol. Chem.*, **258**, 6682–6685.

Sun,X.J., Rothenberg,P., Kahn,C.R., Backer,J.M., Araki,E., Wilden,P.A., Cahill,D.A., Goldstein,B.J. and White,M.F. (1991) Structure of the insulin receptor substrate IRS-1 defines a unique signal transduction protein. *Nature*, **352**, 73–77.

Sun,X.J., Crimmins,D.L., Myers,M.G., Miralpeix,M. and White,M.F. (1993) Pleiotropic insulin signals are engaged by multisite phosphorylation of IRS-1. *Mol. Cell. Biol.*, **13**, 7418–7428.

Tavare,J.M. and Siddle,K. (1993) Mutational analysis of insulin receptor function: consensus and controversy. *Biochim. Biophys. Acta*, **1178**, 21–39.

Tavare,J.M., O'Brien,R.M., Siddle,K. and Denton,R.M. (1988) Analysis of insulin-receptor phosphorylation sites in intact cells by two-dimensional phosphopeptide mapping. *Biochem. J.*, **253**, 783–788.

Taylor,S.S., Radzio-Andzelm,E. and Hunter,T. (1995) How do protein kinases discriminate between serine/threonine and tyrosine? Structural insights from the insulin receptor protein-tyrosine kinase. *FASEB J.*, **9**, 1255–1266.

Tornqvist,H.E., Pierce,M.W., Frackelton,A.R., Nemenoff,R.A. and Avruch,J. (1987) Identification of insulin receptor tyrosine residues autophosphorylated *in vitro*. *J. Biol. Chem.*, **262**, 10212–10219.

Ullrich,A. *et al*. (1985) Human insulin receptor and its relationship to the tyrosine kinase family of oncogenes. *Nature*, **313**, 756–761.

Wei,L., Hubbard,S.R., Hendrickson,W.A. and Ellis,L. (1995) Expression, characterization and crystallization of the catalytic core of the human insulin receptor protein-tyrosine kinase domain. *J. Biol. Chem.*, **270**, 8122–8130.

White,M.F. and Kahn,C.R. (1994) The insulin signaling system. *J. Biol. Chem.*, **269**, 1–4.

White,M.F., Shoelson,S.E., Keutmann,H. and Kahn,C.R. (1988) A cascade of tyrosine autophosphorylation in the β-subunit activates the phosphotransferase of the insulin receptor. *J. Biol. Chem.*, **263**, 2969–2980.

Yamaguchi,H. and Hendrickson,W.A. (1996) Structural basis for activation of human lymphocyte kinase Lck upon tyrosine phosphorylation. *Nature*, **384**, 484–489.

Zheng,J., Trafny,E.A., Knighton,D.R., Xuong,N.H., Taylor,S.S., Ten Eyck,L.F. and Sowadski,J.M. (1993) 2.2 Å refined crystal structure of the catalytic subunit of cAMP-dependent protein kinase complexed with MnATP and a peptide inhibitor. *Acta Crystallogr.*, **D49**, 362–365.